Effect of disorder on superconductivity in the presence of spin-density wave order

Vivek Mishra

Materials Science Division, Argonne National Laboratory, Argonne, Illinois 60439, USA

(Received 19 November 2014; revised manuscript received 27 January 2015; published 2 March 2015)

The majority of unconventional superconductors has close proximity to a magnetic phase. In many cases, the magnetic phase coexists with superconductivity in some fraction of the phase diagram. The response of these two competing phases to disorder can be used as a tool to gain a better understanding of these complex systems. Here I consider the effect of disorder on a multiband superconductor appropriate for the ferro-pnictide superconductors. I consider both interband and intraband scattering for a two-band model consisting of a hole pocket and an electron pocket. The scattering from pointlike impurities is treated within the self-consistent Born approximation. I calculate the effect of disorder on the transition temperature to the superconducting state. The influence of impurity scattering on the low-energy excitation spectrum in the superconducting state is also studied for different kinds of gap structures.

DOI: 10.1103/PhysRevB.91.104501 PACS number(s): 74.20.−z, 74.70.Xa, 74.62.En, 74.25.Jb

I. INTRODUCTION

The coexistence of magnetism and superconductivity is a long-known problem in contemporary physics. Recent discovery of the iron-based superconductors (FeScs) has renewed interest in this old problem. There are some generic features among the various families of FeScs. In general, they have multiple electron and holelike Fermi surfaces. Parent compounds of many families show long-range spin-density wave (SDW) order, which weakens as superconductivity emerges.

The symmetry of the order parameter in these systems is still an unsettled issue. One of the leading candidates for the symmetry of the superconducting gap in the FeScs is the $s_{\pm}$ state, where the electron and the hole Fermi surfaces have the order parameters with opposite signs [1–6]. This kind of state appears in the spin-fluctuation-based pairing theory. On the other hand, a different mechanism, where pairing is mediated by orbital fluctuations, leads to the s_{++} state, which does not have relative sign change of the order parameters between the electron and the hole pockets [7]. Spin-fluctuation-mediated pairing can also lead to accidental nodes or strong anisotropy in the order parameters [8]. Most of the theoretical work has focused on superconductivity. Recently, spin-fluctuation-based calculations have been performed in the SDW state, which predict singlet and triplet superconducting states with the possibility of order-parameter nodes [9,10]. Given the fact that the SDW phase coexists in many FeScs, its role in pairing cannot be ignored. A profound understanding of the interplay between the SDW phase and the superconducting phase is essential to extricate the enigma of the microscopic pairing mechanism and structure of the superconducting order parameter. It is important to comprehend what kind of superconducting state can coexist with the SDW order with a transition temperature of few kelvins, as observed in many FeScs. Another key question is how the structure of the superconducting gap evolves as the SDW phase weakens.

The response of a superconductor to different kinds of impurities strongly depends on the structure of the gap. An *isotropic s*-wave superconductor is immune to nonmagnetic impurity scattering, while magnetic impurities strongly suppress superconductivity [11,12]. In multiband superconductors with isotropic gaps on the individual Fermi surfaces, only the impurities which can mix order parameters with opposite signs suppress superconductivity. However, nonmagnetic impurity scattering lowers the critical temperature (T_c) weakly, if the order parameters have anisotropy even without any sign change. The effects of impurities on superconductivity have been studied heavily, but these effects have not been explored to that degree in the presence of a coexisting order. Fernandes *et al.* have shown that in the coexisting phase of an isotropic $s_{\pm}$ state with the SDW order, T_c can be enhanced by adding impurities [13]. They showed that relatively stronger suppression of the SDW phase enhances superconductivity, which effectively overcomes the pair-breaking effect of disorder in some cases. It should be noted here that the SDW order gets suppressed by both interband and intraband impurity scattering [14]. On the contrary, not all kinds of impurities suppress superconductivity.

Apart from changing the critical temperature, impurities also modify the low-temperature properties of the superconductors. In a fully gapped superconductor, an impurity band inside the gap can give rise to power-law behavior in the thermodynamic and the transport measurements. Impurity scattering can alter the low-temperature behavior of the physical quantities such as penetration depth, thermal conductivity, etc., in the nodal superconductors. Wang *et al.* have proposed an experiment to distinguish between the $s_{\pm}$ and s_{++} state exploiting the effect of disorder [15]. Irradiation techniques to systematically introduce disorder can be used to understand the structure of gap together with other measurements such as the penetration depth or the thermal conductivity. Recently, Mizukami *et al.* [16] used this approach for a P-doped $BaFe_2As_2$ compound, and found evidence for accidental nodes based on the simultaneous use of the electron irradiation technique and penetration depth measurement.

In this paper, I study the effect of disorder on the coexisting phase of the superconductivity and the SDW state, including anisotropy in the superconducting gaps. Earlier work in this area has mostly focused on the effect of disorder on T_c for an isotropic $s_{\pm}$ state [13,14]. I consider the role of anisotropy in the order-parameter structure, which is very likely to happen in

these systems due to the involvement of many different orbitals in the formation of multiple bands. There is also evidence of strong anisotropy and possibilities of accidental nodes in $BaFe_2As_2$-based FeScs. This is one of the most studied family of the FeScs, which is an antiferromagnetic metal in the parent state and in which the superconducting state appears upon doping of the electrons or the holes. Even isovalent doping of P for As leads to the superconductivity. In all of these cases, the underdoped side of the phase diagram shows the coexistence of the SDW phase with the superconducting order. From the experimental perspective, systematic irradiation studies have been performed on both the hole-doped and the electron-doped systems. Van der Beek *et al.* have found suppression of the transition temperature in the electron-doped and P-doped $BaFe_2As_2$ systems, subjected to the electron irradiation [17]. They attributed this to the possibility of three-dimensional nodes. Taen *et al.* studied the effect of electron irradiation on K-doped $BaFe_2As_2$, and found relatively strong suppression of the transition temperature in the underdoped samples compared to the optimally or overdoped samples [18]. Similar results were reported by Cho *et al.* on K-doped $BaFe_2As_2$ systems [19]. They also measured the temperature dependence of the penetration depth in the irradiated samples. In contrast to the optimally doped and overdoped samples, they found evidence for significant anisotropy in the order parameter in the underdoped phase. Therefore, it is important to understand the role of anisotropy in the order parameter to interpret the experimental data. In this work, I study the effect of disorder on an anisotropic superconducting order parameter. I calculate the effect of disorder on the transition temperature and the density of states (DOS), which is directly related to many low-temperature properties of the superconducting state.

This paper is organized as follows: in Sec. II, I describe the model used in this work. In Sec. III, I present the results on the effect of disorder on T_c, and Sec. IV is dedicated to the discussion of the density of state in the presence of impurity scattering. I then conclude in Sec. V.

II. MODEL

I consider a minimal two-band model with cylindrical Fermi surfaces: one for the holelike pocket and one for the electronlike pocket. Raghu *et al.* have shown that the two-band model with electronlike and holelike Fermi-surface sheets is sufficient to describe the low-energy physics of FeScs [20]. I work in the unfolded zone. In the context of the SDW instability, Eremin and Chubukov have shown that only one of the electron pockets and one of the hole pockets participates in the SDW formation [21]. It has been shown in many earlier works that this simple model allows one to capture qualitative features observed in the experiments [22–24]. For the hole and the electron Fermi surfaces, the electronic dispersions read

$$\xi_h(k) = \mu_h - \frac{k^2}{2m_h}, \tag{1}$$

$$\xi_e(k) = \frac{(k_x - Q_x)^2}{2m_x} + \frac{(k_y - Q_y)^2}{2m_y} - \mu_e, \tag{2}$$

where (Q_x,Q_y) is the SDW ordering vector, m_h is the hole mass, $m_{x/y}$ is the electron mass along the $\hat{x}/\hat{y}$ direction, and $\mu_{h/e}$ is the energy offset for the hole/electron band. It is useful to write these dispersions as

$$\xi_h = -\xi, \tag{3}$$

$$\xi_e = \xi + 2\delta. \tag{4}$$

Here, δ is the energy scale, which is a quantitative measure of the deviation from perfect nesting. Perfect nesting is achieved by setting $\delta = 0$. In general, δ is a function of the angle on the Fermi surface and goes to zero on the hotspots. This nesting function δ can be tuned by doping or pressure. For the dispersions considered here,

$$\delta(\phi) = \delta_0 + \delta_1 \cos 2\phi, \tag{5}$$

where ϕ is the angle along the electronlike Fermi surface. The nesting is controlled by two parameters, δ_0 and δ_1. They are the keys to control the nature of the ground state and the phase diagram [22,23]. In this work, the values of δ_0 and δ_1 are chosen to achieve the coexistence of the SDW phase and superconductivity. The model Hamiltonian in the two-band Nambu basis $\Psi^\dagger = (c^\dagger_{k_1\uparrow}, c_{-k_1\downarrow}, c^\dagger_{k_2\uparrow}, c_{-k_2\downarrow})$ reads [22,24]

$$\begin{aligned} \mathbf{H} &= \Psi^\dagger \cdot \mathcal{H} \cdot \Psi, \\ \mathcal{H} &= \begin{bmatrix} \xi_1 & \Delta_1 & M & 0 \\ \Delta_1 & -\xi_1 & 0 & M \\ M & 0 & \xi_2 & \Delta_2 \\ 0 & M & \Delta_2 & -\xi_2 \end{bmatrix}, \end{aligned} \tag{6}$$

where $c^\dagger_{k_i\alpha}$ ($c_{k_i\alpha}$) is the creation (annihilation) operator for the fermions on band $i = 1,2$ with spin $\alpha = \uparrow, \downarrow$. The hole and the electron bands are denoted by subscript indices 1 and 2, respectively. The mean-field self-consistency conditions are

$$\begin{aligned} \Delta_i &= \sum_{j,k,\alpha,\beta} V^{sc}_{ij}(-i\sigma^y)_{\alpha\beta}\langle c_{-k_j\alpha} c_{k_j\beta}\rangle, \\ M &= \sum_{k,\alpha,\beta} V^{sdw}(\sigma^z)_{\alpha\beta}\langle c^\dagger_{k_1\alpha} c_{k_2\beta}\rangle, \end{aligned} \tag{7}$$

where i,j are the band indices and α,β are the spin indices. σ^x, σ^y, and σ^z are the Pauli matrices in the spin space. In the SDW state, long-range SDW order leads to reconstruction of the Fermi surfaces. The resulting Fermi surfaces are defined by the eigenvalues of the Hamiltonian, which read

$$E_\pm = \frac{\xi_h + \xi_e \pm \sqrt{(\xi_e - \xi_h)^2 + 4M^2}}{2}. \tag{8}$$

Figure 1 shows the reconstructed bands. For large value of the SDW order parameter, only the pockets corresponding to E_- cross the Fermi energy.

At the transition to the superconducting state, only the first-order terms in the superconducting order parameters are retained. This reduces the T_c determination problem to an eigenvalue problem for a $n \times n$ matrix, where n is the number of order parameters. The coefficients of this pairing matrix depend on the details of interactions, underlying electronic structure, and various scattering processes. In the presence of the SDW order, the coefficients of the pairing matrix are calculated using the SDW state Green's function, which

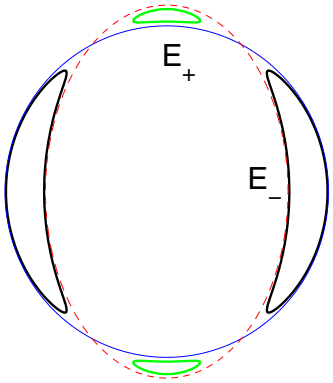

FIG. 1. (Color online) Schematic plot of the Fermi surfaces. Thin lines show the Fermi surfaces in the paramagnetic state, where the solid line represents the holelike Fermi surface and the dashed line shows the shifted electron Fermi surface. Thick lines represent the pockets corresponding to the reconstructed bands in the SDW state.

carries the information about the reconstruction of the Fermi surfaces. The interaction for the SDW order V_{sdw} is assumed to be momentum independent. Pairing interactions for the superconductivity are

$$V_{ij}^{sc} = V_{ij}^{0}\mathcal{Y}_i(\phi_i)\mathcal{Y}_j(\phi_j). \tag{9}$$

Here, ϕ_i is the angle along the ith band. These interactions lead to an isotropic order parameter on the hole pocket and an anisotropic order parameter on the electron pocket in the absence of the SDW order parameter, which reads

$$\Delta_h = -\Delta_1\mathcal{Y}_h, \tag{10}$$

$$\Delta_e = \Delta_2\mathcal{Y}_e, \tag{11}$$

where

$$\mathcal{Y}_h = 1, \tag{12}$$

$$\mathcal{Y}_e = (1 + r\cos 2\phi). \tag{13}$$

There is a relative sign change between the average values of the order parameters on the two bands. These interactions are purely phenomenological to get the desired order-parameter anisotropy in the pure superconducting state. In general, an isotropic interaction can become strongly momentum dependent on the reconstructed Fermi surfaces [25,26]. For momentum-independent gaps and interactions, it is easier to understand the relation between the fermions in the paramagnetic state and in the ordered SDW state. A simple $s_{\pm}$ state transforms into nodeless gaps on the resulting Fermi surfaces; on the other hand, the s_{++} state gives rise to nodes in the SDW state [25,27]. Later, in Sec. IV, I discuss the DOS in the coexisting phase, which contains the information about nodes of the order parameter on the reconstructed Fermi surfaces. In the next section, I discuss the importance of anisotropy in the the context of T_c.

A. Effect of anisotropy on T_c

Anisotropy of the superconducting order parameter on the electron pocket is controlled by the parameter r [see Eq. (13)]. Recent theoretical studies have found many different kinds of order parameters including gap nodes in the coexisting phase [9,10]. These studies are based on spin-fluctuation-mediated pairing in the SDW phase and they predict pairing instabilities in both of the spin channels, i.e., singlet and triplet. Here I consider only singlet pairing. Different possible gap structures are modeled using phenomenological interactions. In the presence of the SDW order, the structure of the gap relative to hotspots becomes critical. To get a qualitative understanding of it, I consider a simple two-parameter interaction potential with equal attractive intraband pairing interactions, $V_{ij}^{0} = -\lambda_0$, and a repulsive interband interaction,

$$V_{eh}^{0} = V_{he}^{0} = \rho\lambda_0, \tag{14}$$

where ρ controls the strength of the interband coupling compared to the intraband coupling λ_0. All of the energy scales are measured in the unit of T_{c0}, which is the superconducting transition temperature in the absence of the SDW order. The SDW transition temperature (T_{s0}) with perfect nesting is $5T_{c0}$ for the SDW interaction (V_{sdw}) chosen here. In order to study the effect of the disorder on T_c, I keep the Fermi surface unchanged (i.e., δ), which fixes the SDW transition temperature. Since superconductivity does not exist with perfect nesting, I take $\delta_0 = 1.068T_{s0}$ and $\delta_1 = 1.257T_{s0}$, which allows the coexistence of superconductivity with the SDW phase. Due to deviation from the perfect nesting, the SDW transition temperature (T_s) also reduces to $2.5T_{c0}$ from its perfect nesting value T_{s0}. Figure 2 shows the critical temperature as a function of anisotropy parameter r and relative strength of interband interaction ρ. For the phase diagram shown in Fig. 2, the value of the intraband interaction is chosen such that the critical temperature is the same in the entire phase diagram in the absence of SDW order. For weaker interband interaction, T_c is sensitive to its strength, but its value saturates

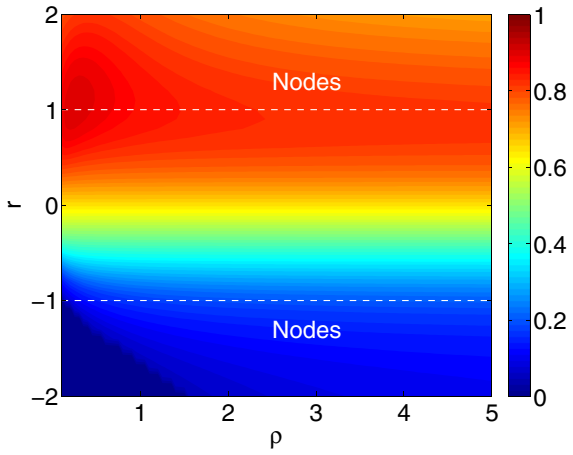

FIG. 2. (Color online) Transition temperature as a function of order-parameter anisotropy parameter r and the relative strength of the interband coupling ρ. Regions with nodal superconductivity in the absence of the SDW state are indicated in the phase diagram ($r \geqslant 1$ and $r \leqslant -1$). The transition temperature is set to unity for the entire parameter space in the absence of the SDW order.

with increasing interband coupling. The suppression of T_c is highest when the gap nodes or the gap minima are away from the hotspots, which happens for $r < 0$. By gap minima or nodes, I mean the minimum or node of the gap in the absence of the SDW order. In the presence of the SDW, even a nodal gap structure may become nodeless on the reconstructed Fermi surface, and vice versa. On the other hand, suppression is quite weak when the nodes or minima are near the hotspots ($r > 0$). This behavior is expected because along the hotspots the SDW correlations are very strong. If the gap nodes/minima are away from the hotspots, then the maximum of the superconducting order parameter is located near the hotspots, which faces stern competition from the SDW order parameter. This is in contrast to the case when the maximum of the gap is away from the hotspots and the nodes/minima are near it. In this situation, superconductivity is weakest on the regions of the Fermi surface, where the SDW correlations are maximized, and hence two phases coexist easily. This is qualitatively true irrespective of the strength of the interband coupling. Next, I discuss the basic formalism for the treatment of the disorder due to randomly distributed pointlike impurities.

B. Model for disorder

To understand the effect of disorder, I focus on three representative cases, with $r = 0$ and $r = \pm 1.3$. In the absence of SDW order, an isotropic $s_\pm$ state is realized for $r = 0$ and $|r| = 1.3$ gives an anisotropic $s_\pm$ state with accidental nodes. The nodes are located near the hotspots for $r = 1.3$, and away from them for $r = -1.3$. In this work, only nonmagnetic pointlike impurities are considered. A general impurity potential for a nonmagnetic pointlike scatterer in the two-band Nambu basis reads

$$\mathbf{U} = \begin{bmatrix} u_1 & 0 & v & 0 \\ 0 & -u_1 & 0 & -v \\ v & 0 & u_2 & 0 \\ 0 & -v & 0 & -u_2 \end{bmatrix}, \tag{15}$$

where u_i is the intraband scattering potential for the ith band and v is the interband scattering potential. One should note that the notion of the interband and the intraband scattering introduced here refers to the nature of impurity scatterings in the paramagnetic state. In the SDW phase, reconstruction of the Fermi surfaces takes place. In the reconstructed Fermi-surface pockets, both the interband and intraband scattering are possible and their amplitude will depend on the impurity potentials in the paramagnetic state. The effect of reconstruction of Fermi surfaces is built into this framework and taken into account in calculating the effect of impurities by using the Green's function, which involves the SDW order. The amount of impurity scattering is quantified in terms of the total normal-state (paramagnetic-state) scattering rate (Γ), which can be extracted from the shift of the resistivity curves in the experiments. This approach allows one to compare the effect of impurities in systems with and without the coexisting SDW order. To keep the number of free parameters to a minimum, I take same intraband scattering potentials for both bands ($u_1 = u_2 = u$). This assumption does not change any of the qualitative conclusions. The interband scattering v is varied and its strength is controlled with a dimensionless parameter α. The interband scattering potential reads

$$v = \alpha u. \tag{16}$$

The effect of impurity scattering is included through the self-energy calculated within the self-consistent Born approximation. The self-energy is

$$\Sigma = n_{imp} \sum_k \mathbf{U} \cdot \mathbf{G} \cdot \mathbf{U}, \tag{17}$$

where n_{imp} is the impurity concentration and $\mathbf{G}$ is the impurity dressed Green's function defined as

$$\mathbf{G}^{-1} = \mathbf{G}_0^{-1} - \Sigma, \tag{18}$$

$$\mathbf{G}_0^{-1} = i\omega \mathbb{1} - \mathcal{H}, \tag{19}$$

where $\mathbb{1}$ is the identity matrix in the two-band Nambu basis. I use the standard trick of replacing all of the quantities in the Green's function by disorder renormalized quantities,

$$\tilde{\omega}_1 = \omega + i(\Sigma_{11} + \Sigma_{22})/2, \tag{20}$$

$$\tilde{\omega}_2 = \omega + i(\Sigma_{33} + \Sigma_{44})/2, \tag{21}$$

$$\tilde{M}_1 = M + (\Sigma_{13} + \Sigma_{24})/2, \tag{22}$$

$$\tilde{\Delta}_1 = \Delta_1 + \Sigma_{12}, \tag{23}$$

$$\tilde{\Delta}_2 = \Delta_2^{\text{iso}} + \Sigma_{34}, \tag{24}$$

where Σ_{mn} is the (m,n) element in the 4×4 self-energy matrix Σ, and Δ_2^{iso} is the isotropic component of the order parameter in the electron band. Equations (17)–(24) are solved self-consistently using the iteration method.

III. SUPPRESSION OF CRITICAL TEMPERATURE

To compare the suppression of T_c for different kinds of gaps, the transition temperature is kept the same in the absence of the SDW order for all of the values of r considered here. Figure 3 shows the variation of T_c as a function of total impurity scattering rate (Γ) in the normal state and it is measured in the unit of T_{c0}. For each case the strengths of the impurity potentials are kept fixed, and impurity concentration (n_{imp}) is tuned to change Γ. With only intraband scattering, T_c enhances with increasing disorder, as shown in Fig. 3(a). The enhancement rate is higher for the states, which suffer stronger damage due to the SDW state. For the state with gap nodes near the hotspots, the variation of T_c is very weak. This enhancement is resulting from the suppression of the SDW state due to pure intraband impurity scattering. The intraband scattering is a strong pair breaker for the SDW state, and suppresses superconductivity only if the order parameter is anisotropic on the Fermi surface. *The Anderson's theorem still holds in the presence of the SDW order*, and it is clear that the ordinary nonmagnetic impurities do not cause pair breaking for the *isotropic* gaps. As the interband scattering increases, the rate of T_c enhancement decreases, as shown in Fig. 3(b). For the $r = 1.3$ state, the T_c now start to decrease, which

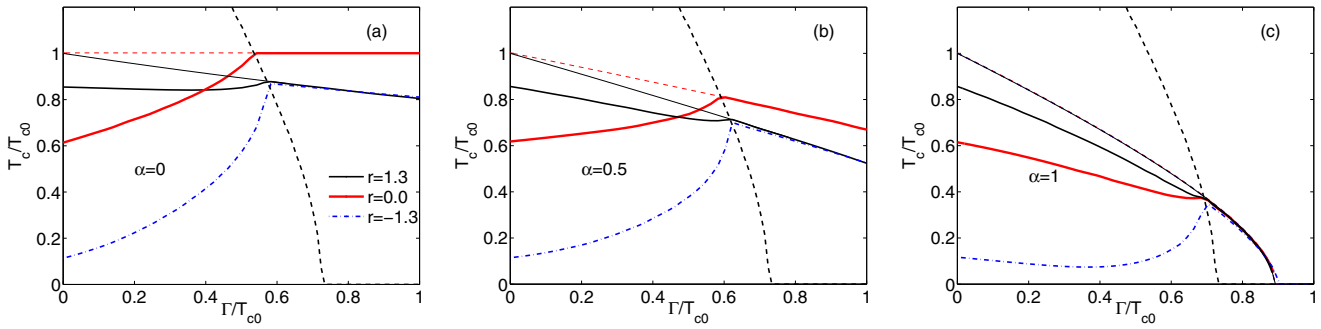

FIG. 3. (Color online) Transition temperature as a function of total normal state impurity scattering rate (Γ) for different kinds of order parameters. The relative strength of the interband scattering rate is denoted by α and its value is indicated in each panel. The thick dashed black line is representing the SDW transition temperature and thin dashed and solid lines are T_c for the superconducting state without the SDW order for $r = 0$ and $r = \pm 1.3$, respectively. All energy scales are measured in the unit of T_{c0}, which is the superconducting transition temperature in the absence of the SDW order and kept same for all three order parameters.

was least affected by pure intraband scattering. This happens because finite interband impurity scattering causes more pair breaking. The amount of pair breaking increases with a rise in the interband scattering. Figure 3(c) shows the T_c when the interband scattering is as strong as the intraband scattering. In this case, T_c also decreases for the isotropic $s_\pm$ state. The decrease in T_c is minimal for $r = -1.3$, when nodes are located away from the hotspots. In this case, T_c increases near the disappearance of the SDW order. For a specific value of the impurity scattering rate, the transition to the SDW phase and the superconducting phase occurs simultaneously at a temperature $T_{\rm cross}$. Whenever the clean limit T_c is smaller than $T_{\rm cross}$, the superconducting transition temperature increases with the disorder, although the T_c may increase nonmonotonically. In Fig. 3(c), for $r = 0$ and $r = 1.3$, this simultaneous transition happens at a temperature below the clean limit T_c for isotropic impurity scattering, and hence T_c decreases with the disorder in the coexisting phase; also, on the contrary, for $r = -1.3$, this crossing is higher than the clean limit T_c, so T_c increases with the weakening of the SDW phase due to the impurity scattering. There is a weak suppression of T_c in this case for low disorder. This happens because isotropic impurities are also suppressing superconductivity, but for moderate disorder the enhancement of superconductivity is not able to overcome the pair-breaking effect of the impurities. There are two competing phenomena taking place in the coexisting phase. First is the direct effect of the disorder on T_c, which is the suppression of superconductivity, and the secondary effect is the enhancement of T_c due to the suppression of the competing SDW state. Depending on the strength of the pair-breaking component of the impurity scattering, either of these effects can win, which may lead to an increase or a decrease of T_c. In the next section, I present the effect of disorder on the low-energy density of states, which directly reflects in many physical properties at the low temperatures.

IV. DENSITY OF STATES

The low-energy quasiparticle excitation spectrum reflects in the thermodynamic and the transport properties of the superconductors. This is not only sensitive to the structure of the order parameter near the Fermi surface but also to the impurity scattering. In the case of a d-wave superconductor, the linear density of states becomes a quadratic function of energy with increasing disorder. For systems with accidental nodes, dominant intraband scattering leads to an energy gap in the excitation spectrum [28]. How does the presence of the SDW order affect the low-energy DOS, and how does it change due to the impurity scattering? These are the important questions to answer. In order to calculate the DOS, the full Green's function is needed in the real frequencies. The analytic continuation from the Matsubara frequencies is done with an artificial broadening of $0.025T_{c0}$. The order parameters are calculated at $T = 0.1T_c$ by solving the self-consistency equations including the effect of the impurities. In the subsequent sections, I discuss the disorder effect on the DOS for each case considered in this paper.

A. Isotropic $s_\pm$ state

The DOS for the isotropic $s_\pm$ state is shown in Fig. 4 for pure intraband impurity scattering. In the presence of the SDW order for an isotropic $s_\pm$ superconductor, there is always an energy gap near the Fermi surface. One should further note that in general the DOS is particle-hole asymmetric.

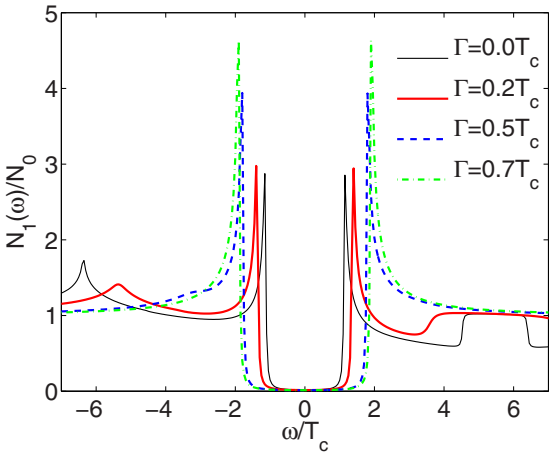

FIG. 4. (Color online) Density of states for a system with isotropic $s_\pm$ state and pure intraband impurity scattering, for various values of the total normal-state impurity scattering rate Γ.

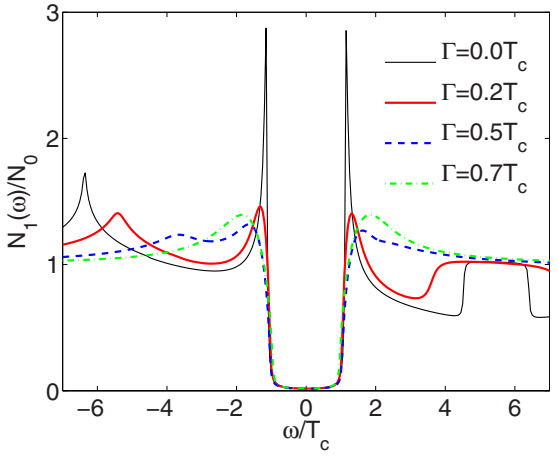

FIG. 5. (Color online) Density of states of a system with isotropic $s_\pm$ state and moderate interband scattering ($\alpha = 0.5$), for different values of the total normal-state impurity scattering rate Γ.

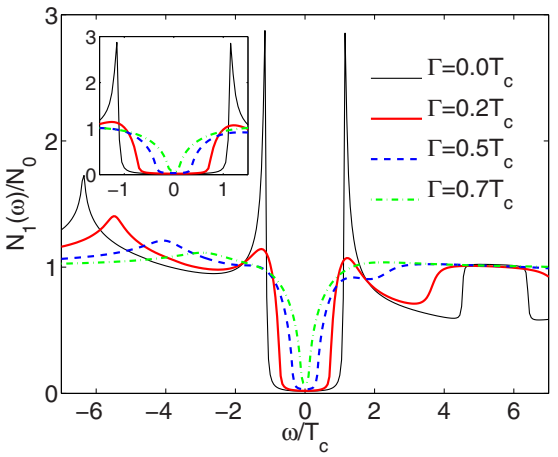

FIG. 6. (Color online) Density of states of a system with isotropic $s_\pm$ state and isotropic impurity scattering ($\alpha = 1$), for different values of the total normal-state impurity scattering rate Γ. Inset: The low-energy DOS is shown more clearly for the same case.

The structures in the DOS above $|\omega| > 2T_c$ are related to the SDW order and move towards the lower energies as the superconducting order becomes stronger. For pure intraband disorder, the SDW phase becomes weaker with increasing disorder. Since there is not much difference between the two bands, I therefore show the results for only one of the bands. Since the intraband scattering is not pair breaking for the isotropic $s_\pm$ state, the superconducting phase gets stronger with more impurities, which reflects as a larger gap in the DOS with increasing disorder. In fully gapped superconductors, pair-breaking impurities can give rise to tail states [29–31]. These states cannot be captured within the Born approximation. Since these tail states make a very small contribution to the DOS, they do not qualitatively change any of the results. The addition of interband scattering changes this picture because it also suppresses superconductivity. Figure 5 shows the DOS for the isotropic $s_\pm$ with the SDW state with moderate interband impurity scattering. For Fig. 5, the strength of the interband impurity potential is half of the intraband scattering potential. With finite pair-breaking scattering, the superconducting order does not recover its clean limit value. However, the DOS becomes more and more particle-hole symmetric with diminishing SDW order. Further increase in the interband scattering causes more pair breaking. In the limit of the isotropic impurity scattering, when both the intraband and the interband scattering are equally strong, both of the orders get suppressed. Depending upon the strength of interband scattering, the effective gap in the DOS becomes very small due to the formation of a midgap impurity band, as shown in Fig. 6. Stronger interband scattering leads to the annihilation of both of the orders, which is shown in Fig. 6. It should be noted here that a small effective gap may lead to strong deviation from the usual activated behavior observed in some physical properties. Such small gaps can change the low-temperature exponential behavior into a power law in the temperature dependence of the penetration depth or thermal conductivity. The inset in Fig. 6 highlights the energy range in the DOS, which has a strong influence on the low-temperature properties.

B. Nodes near the hotspots

Figure 7 shows the DOS for a state with accidental nodes located near the hotspots without SDW order on the electronlike Fermi surface with only intraband impurity scattering. Even in the clean limit, the DOS is fully gapped. Due to reconstruction of the Fermi surfaces in the SDW phase, the regions near the hotspots become gapped. This reconstruction of the Fermi surface leads to the disappearance of the nodes, otherwise located on the Fermi surface in the absence of the SDW energy gap. Similar to the case of the $s_\pm$ state, the DOS is particle-hole asymmetric. The gap size reduces with increase in disorder, but there is a small gap even after the extinction of the SDW order, as shown in Fig. 7. This is consistent with disorder-driven node lifting [28]. The addition of the interband scattering gives rise to midgap impurity bands and the effective gap steadily shrinks with the accumulation of impurities. Interband scattering hinders

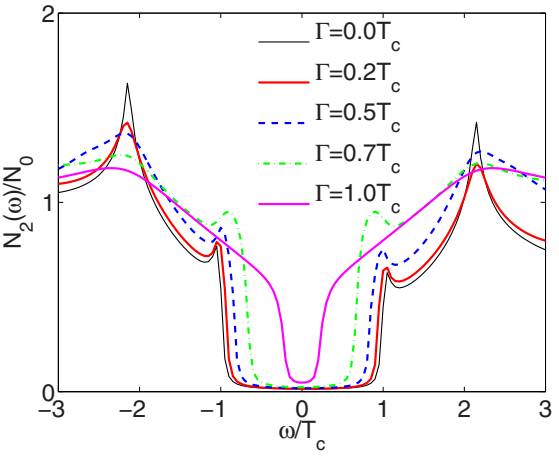

FIG. 7. (Color online) Density of states for a system with accidental nodes located near the hotspots on the electronlike Fermi surface in the absence of the SDW order, with only intraband impurity scattering for various values of disorder.

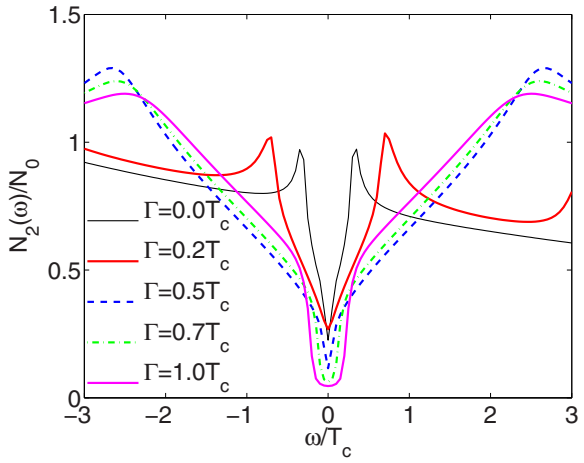

FIG. 8. (Color online) Density of states for a system with accidental nodes located away from the hotspots on the electronlike Fermi surface in the absence of the SDW order, with only intraband impurity scattering for various values of disorder.

the node-lifting phenomena. The possibility of node lifting depends on the degree of anisotropy in the order parameter. For smaller values of r, the nodes get lifted with a moderate amount of the intraband scattering, while larger r values require stronger intraband scattering. For the band with an isotropic gap, the DOS is qualitatively similar to the isotropic $s_{\pm}$ case, with only intraband scattering.

C. Nodes away from the hotspots

When the order-parameter nodes are located far away from the hotspots, they survive the Fermi-surface reconstruction, which gaps the regions near the hotspots. In such systems with no disorder, the nodes in the superconducting gap give rise to linear DOS near the Fermi energy. As illustrated in Fig. 8, as the impurity scattering increases, the sharp peaks in the DOS get smeared and the DOS becomes more particle-hole symmetric. Figure 8 shows the DOS for this case with only intraband impurity scattering. The DOS at the Fermi energy first increases and then disappears. This is similar to the behavior shown by superconducting states with accidental nodes for pure intraband scattering [28]. Like the previous case, depending on the amount of the anisotropy in the gap (magnitude of r), nodes may disappear once the SDW order vanishes. This happens in the case considered here. So the qualitative behavior of nodes on the reconstructed Fermi surface is the same as it would be without the SDW order.

V. CONCLUSION

In this work, I studied the effect of disorder on the superconducting transition temperature in the presence of competing SDW order. I considered both the interband and the intraband impurity scattering processes for several candidates of order parameters, appropriate for the iron pnictides. I showed that both the enhancement and the suppression of the critical temperature are possible in the coexisting phase. The anisotropy in the order parameter of a superconductor plays an important role in its response to impurities. The anisotropy is also critical in determining the transition temperature in the coexisting phase. The transition temperatures for systems in which the order-parameter nodes/minima are located near the hotspots are higher than those of systems in which the nodes/minima are far from the hotspots. The reason for enhancement of T_c with the addition of the disorder is due to the suppression of the SDW order. The enhancement becomes weaker as the pair-breaking component for the superconductivity order (i.e., interband scattering) increases. This is also sensitive to the relative strength of the SDW and the superconducting instabilities in the clean system. In a realistic situation, systematic insertion of impurities will lead to suppression of both of the orders because the realistic impurities have both the intraband and the interband scattering components and the order parameters have anisotropy.

I also discussed the effect of disorder on the low-energy density of states. In the presence of the SDW order, the DOS remains gapped at the Fermi surface unless the nodes are located away from the hotspots. The DOS is particle-hole asymmetric due to the presence of the SDW order. Impurity scattering suppresses the SDW order and the degree of particle-hole asymmetry decreases. For pure intraband scattering, an isotropic $s_{\pm}$ system remains gapped at the Fermi level and the effective gap in the DOS increases with more disorder. For states with accidental nodes surviving in the Fermi-surface reconstruction, the DOS is linear near the Fermi energy. Increasing disorder lifts the nodes as in the case of a pure superconducting state. If the anisotropy is large and the amount of disorder that kills the SDW phase is not sufficient to lift the nodes, then the gap will be absent in the DOS and nodes will disappear at higher disorder. The interband scattering slows down the node lifting. For an isotropic $s_{\pm}$ system, moderate interband scattering lowers the gap in DOS and strong interband scattering very quickly kills the gap. This may give rise to power-law behavior in the temperature dependence of the penetration depth or the thermal conductivity. A more systematic study on this line is in progress and will be reported elsewhere.

ACKNOWLEDGMENTS

I thank Alexei Koshelev and Maxime Leroux for useful discussions. This work was supported by the Center for Emergent Superconductivity, an Energy Frontier Research Center funded by the U.S. Department of Energy, Office of Science, under Award No. DE-AC0298CH1088.

[1] D. C. Johnston, Adv. Phys. **59**, 803 (2010).
[2] P. C. Canfield and S. L. Bud'Ko, Annu. Rev. Condens. Matter Phys. **1**, 27 (2010).
[3] P. J. Hirschfeld, M. M. Korshunov, and I. I. Mazin, Rep. Prog. Phys. **74**, 124508 (2011).
[4] G. R. Stewart, Rev. Mod. Phys. **83**, 1589 (2011).

[5] H.-H. Wen and S. Li, Annu. Rev. Condens. Matter Phys. **2**, 121 (2011).
[6] A. Chubukov, Annu. Rev. Condens. Matter Phys. **3**, 57 (2012).
[7] S. Onari and H. Kontani, Phys. Rev. Lett. **103**, 177001 (2009).
[8] S. Graser, T. A. Maier, P. J. Hirschfeld, and D. J. Scalapino, New J. Phys. **11**, 025016 (2009).
[9] J. Schmiedt, P. M. R. Brydon, and C. Timm, Phys. Rev. B **89**, 054515 (2014).
[10] W. Rowe, I. Eremin, A. Rømer, B. M. Andersen, and P. J. Hirschfeld, arXiv:1312.1507.
[11] P. Anderson, J. Phys. Chem. Solids **11**, 26 (1959).
[12] A. A. Abrikosov and L. P. Gorkov, Sov. Phys. JETP **12**, 1243 (1961).
[13] R. M. Fernandes, M. G. Vavilov, and A. V. Chubukov, Phys. Rev. B **85**, 140512 (2012).
[14] M. G. Vavilov and A. V. Chubukov, Phys. Rev. B **84**, 214521 (2011).
[15] Y. Wang, A. Kreisel, P. J. Hirschfeld, and V. Mishra, Phys. Rev. B **87**, 094504 (2013).
[16] Y. Mizukami, M. Konczykowski, Y. Kawamoto, S. Kurata, S. Kasahara, K. Hashimoto, V. Mishra, A. Kreisel, Y. Wang, P. J. Hirschfeld, Y. Matsuda, and T. Shibauchi, Nat. Commun. **5**, 5657 (2014).
[17] C. J. van der Beek, S. Demirdiş, D. Colson, F. Rullier-Albenque, Y. Fasano, T. Shibauchi, Y. Matsuda, S. Kasahara, P. Gierlowski, and M. Konczykowski, J. Phys.: Conf. Ser. **449**, 012023 (2013).
[18] T. Taen, F. Ohtake, H. Akiyama, H. Inoue, Y. Sun, S. Pyon, T. Tamegai, and H. Kitamura, Phys. Rev. B **88**, 224514 (2013).
[19] K. Cho, M. Konczykowski, J. Murphy, H. Kim, M. A. Tanatar, W. E. Straszheim, B. Shen, H. H. Wen, and R. Prozorov, Phys. Rev. B **90**, 104514 (2014).
[20] S. Raghu, X.-L. Qi, C.-X. Liu, D. J. Scalapino, and S.-C. Zhang, Phys. Rev. B **77**, 220503(R) (2008).
[21] I. Eremin and A. V. Chubukov, Phys. Rev. B **81**, 024511 (2010).
[22] A. B. Vorontsov, M. G. Vavilov, and A. V. Chubukov, Phys. Rev. B **81**, 174538 (2010).
[23] R. M. Fernandes and J. Schmalian, Phys. Rev. B **82**, 014521 (2010).
[24] A. B. Vorontsov, M. G. Vavilov, and A. V. Chubukov, Phys. Rev. B **79**, 060508 (2009).
[25] S. Maiti, R. M. Fernandes, and A. V. Chubukov, Phys. Rev. B **85**, 144527 (2012).
[26] J.-P. Ismer, I. Eremin, E. Rossi, D. K. Morr, and G. Blumberg, Phys. Rev. Lett. **105**, 037003 (2010).
[27] D. Parker, M. G. Vavilov, A. V. Chubukov, and I. I. Mazin, Phys. Rev. B **80**, 100508 (2009).
[28] V. Mishra, G. Boyd, S. Graser, T. Maier, P. J. Hirschfeld, and D. J. Scalapino, Phys. Rev. B **79**, 094512 (2009).
[29] A. V. Balatsky and S. A. Trugman, Phys. Rev. Lett. **79**, 3767 (1997).
[30] A. V. Shytov, I. Vekhter, I. A. Gruzberg, and A. V. Balatsky, Phys. Rev. Lett. **90**, 147002 (2003).
[31] A. Glatz and A. E. Koshelev, Phys. Rev. B **82**, 012507 (2010).